JOC Article

Theoretical Study of Nucleophilic Substitution at the Disulfide Bridge of Cyclo-L-cystine

Steven M. Bachrach* and Adam C. Chamberlin

Department of Chemistry, Trinity University, 715 Stadium Drive, San Antonio, Texas 78212

sbachrach@trinity.edu

Received January 15, 2003

The reaction of cyclo-L-cystine with thiolate is examined at the B3LYP/6-31+G* level. The two isomers of cyclo-l-cystine differ in their dihedral angle about the disulfide bond; the ***M*** isomer (with dihedral angle of −90.1°) is found to be slightly lower in energy. The nucleophilic substitution reaction at sulfur follows the addition−elimination mechanism, exemplified by the hypercoordinate sulfur intermediate on the reaction surface. The reaction is exergonic ($\Delta G = -6.16$ kcal mol^{-1}), and both the entrance and exit transition state lie below the reactant energies.

Introduction

The thiol−disulfide exchange is one of the fastest reactions in biological systems.[1] An important example is the process of protein folding assisted by protein disulfide isomerase (PDI).[2−4] PDI catalyzes the formation of disulfide bonds via thiolate−disulfide exchange, allowing for a cascade of disulfide formations and cleavages to enable the protein to fold properly. Mixed disulfides formed from proteins are useful in characterizing protein structure and as protecting groups.[5,6] These mixed disulfides are readily generated via the reaction protein−SH + RSSR → protein−S−S−R + RSH. The added benefit is that the original protein can be regenerated by the reverse reaction. Recent examples of the application of this technology are in the modulation of enzymatic activity of ribonuclease A,[7] the determination of the sequence of disulfide bond formation in the folding of ribonuclease A,[8] and in the determination of the distance between thiols in myosin subfragment 1.[9]

We have been examining the nature of the thiolate−disulfide exchange using a computational approach.[10,11] Surprisingly, the simple prototype examples (reactions 1−3, the starred atom is the center under attack) proceed by an addition−elimination (A−E) mechanism, and not the expected S_N2 pathway as found for substitution at carbon,[12] nitrogen,[13] and oxygen.[14] The S_N2 mechanism is observed for the reactions at the Hartree−Fock level, but all computations that involve some accounting for electron correlation (MP2, CCSD, and B3LYP) predict the A−E mechanism. The A−E mechanism is found for substitution of trisulfides[15] and monosulfides[16] as well.

$$HS^- + HS^*SH \rightarrow HSS^*H + HS^- \quad (1)$$

$$MeS^- + HS^*SMe \rightarrow MeSS^*H + MeS^- \quad (2)$$

$$HS^- + MeS^*SH \rightarrow HSS^*Me + HS^- \quad (3)$$

The A−E gas-phase potential energy surface is characterized as a triple-well. The nucleophile and disulfide first combine to form a stable ion−dipole complex. The nucleophile then attacks the disulfide passing through the first transition state (TS) to form a stable intermediate. In the next step, the original disulfide bond cleaves, passing through a second TS to give the product ion−dipole complex. An extreme example of this A−E process is the reaction of chloride with SCl_2; here the intermediate SCl_3^- is so stable that it forms without any barrier, leading to a potential energy surface characterized by just a single critical point, SCl_3^-.[17]

(1) Raines, R. T. *Nat. Struct. Biol.* **1997**, *4*, 424−427.
(2) Noiva, R.; Lennarz, W. J. *J. Biol. Chem.* **1992**, *267*, 3553−3556.
(3) Ruddon, R. W.; Bedows, E. *J. Biol. Chem.* **1997**, *272*, 3125−3128.
(4) Gilbert, H. F. *J. Biol. Chem.* **1997**, *272*, 29399−29402.
(5) Wynn, R.; Richards, F. M. *Methods Enzymol.* **1995**, *251*, 351−356.
(6) Faulstich, H.; Heintz, D. *Methods Enzymol.* **1995**, *251*, 357−366.
(7) Messmore, J. M.; Holmgren, S. K.; Grilley, J. E.; Raines, R. T. *Bioconjugate Chem.* **2000**, *11*, 408−413.
(8) Ruoppolo, M.; Vinci, F.; A., K. T.; Raines, R. T.; Marino, G. *Biochemistry* **2000**, *39*, 12033−12042.
(9) Kliche, W.; Pfannstiel, J.; Tiepold, M.; Stoeva, S.; Faulstich, H. *Biochemistry* **1999**, *38*, 10307−10317.
(10) Bachrach, S. M.; Mulhearn, D. C. *J. Phys. Chem.* **1996**, *100*, 3535−3540.
(11) Bachrach, S. M.; Hayes, J. M.; Dao, T.; Mynar, J. L. *Theor. Chem. Acc.* **2002**, *107*, 266−271.
(12) (a) Gronert, S. *J. Am. Chem. Soc.* **1991**, *113*, 6041−6048. (b) Glukhovtsev, M. N.; Pross, A.; Radom, L. *J. Am. Chem. Soc.* **1996**, *118*, 6273−6284. (c) Bickelhaupt, F. M. *J. Comput. Chem.* **1999**, *20*, 114−128.
(13) (a) Bühl, M.; Schaefer, H. F., III. *J. Am. Chem. Soc.* **1993**, *115*, 364−365. (b) Bühl, M.; Schaefer, H. F., III. *J. Am. Chem. Soc.* **1993**, *115*, 9143−9147. (c) Glukhovtsev, M. N.; Pross, A.; Radom, L. *J. Am. Chem. Soc.* **1995**, *117*, 9012−9018. (d) Gareyev, R.; Kato, S.; Bierbaum, V. M. *J. Am. Soc. Mass Spectrom.* **2001**, *12*, 139−143. (e) Yi, R.; Basch, H.; Hoz, S. *J. Org. Chem.* **2002**, *67*, 5891−5895.
(14) (a) Beak, P.; Loo, D. *J. Am. Chem. Soc.* **1986**, *108*, 3834. (b) Bachrach, S. M. *J. Org. Chem.* **1990**, *55*, 1016−1019. (c) Kurtzweil, M. L.; Beak, P. *J. Am. Chem. Soc.* **1996**, *118*, 3426−3434. (d) Ren, Y.; Wolk, J. L.; Hoz, S. *Int. J. Mass Spectrom.* **2002**, *220*, 1−10.
(15) Mulhearn, D. C.; Bachrach, S. M. *J. Am. Chem. Soc.* **1996**, *118*, 9415−9421.
(16) Bachrach, S. M.; Gailbreath, B. D. *J. Org. Chem.* **2001**, *66*, 2005−2010.
(17) Gailbreath, B. D.; Pommerening, C. A.; Bachrach, S. M.; Sunderlin, L. S. *J. Phys. Chem. A* **2000**, *104*, 2958−2961.

10.1021/jo034046x CCC: $25.00
Published on Web 05/01/2003

We recently reported a computational study of the gas-phase reaction of thiolate with cyclic disulfides.[18] The larger five- and six-membered rings again follow the A−E mechanism. However, the very small three- and four-membered disulfide rings undergo nucleophilic substitution by an S_N2 pathway; their large ring strain cannot accommodate the addition of another bond to sulfur, and therefore, the ring cleaves when attacked by a nucleophile.

We now extend these studies to a more protein-like environment. Cyclo-L-cystine **1** is the smallest peptide that contains a disulfide bridge. While this simple disulfide is not representative of the more usual peptide conformations, it does offer the computational advantage of its limited conformational flexibility. Furthermore, **1** is structurally related to the fungal metabolite gliotoxin **2**,[19] which does undergo nucleophilic attack by glutathione.[20] We report here a computational study of the attack of **1** by thiolate as a guide and model for understanding nucleophilic attack at disulfides in proteins and gliotoxin and its related toxins.

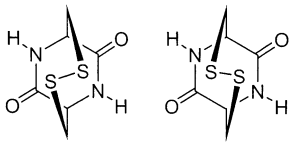

1*P* **1*M***

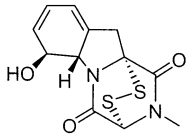

2

Computational Methods

Our previous studies of nucleophilic substitution at sulfur have indicated that electron correlation is necessary to obtain the proper topology of the potential energy surface.[10,11,15] At the Hartree−Fock level, the surface has two wells, corresponding to entrance and exit ion−dipole complexes, and a single TS connecting them—a classic gas-phase S_N2 reaction.[21] However, the MP2, MP4, CCSD, and B3LYP surfaces all have three wells (an A−E mechanism), corresponding to two ion−dipole complexes and an intermediate. The well depths and barrier heights are only slightly dependent on the method, so we chose to employ the B3LYP method here on the basis of its superior computational performance.

All structures were completely optimized at the B3LYP/6-31+G* level;[22] the augmented basis set is necessary to adequately describe anions.[23] Analytical frequencies were determined to characterize the nature of these geometries and to determine zero-point energies and free energies. The ZPEs and vibrational frequencies are used unscaled. Free energies were computed at 298 K using standard partition-function approximations.[24] All calculations were performed using GAUSSIAN-98.[25]

Results and Discussion

Structure of Cyclo-L-cystine 1. Cyclo-L-cystine **1** is a relatively constrained molecule, due to its bicyclic geometry and the two amide groups. However, it was recognized that two configurations are possible, differing in the dihedral angle about the disulfide bridge. The dihedral angle about a disulfide bond is typically about 90°,[26] and the two configurations here are labeled ***P*** for having a positive dihedral (approximately +90°) and the other isomer is labeled ***M*** for having a negative (minus) dihedral (approximately −90°). Spectrometric studies in the 1970s suggested that **1*P*** is the more stable isomer.[27,28] A conformational analysis using molecular mechanics suggested that **1*M*** is slightly more stable (0.3 kcal mol^{-1}) and has about three times as many low-lying conformations than **1*P***.[29] The X-ray crystal structure was reported in 1981,[30] finding the **1*M*** configuration with a dihedral angle about the disulfide bond of −94°.

We optimized the structures of both configurations, and these are shown in Figure 1. Important geometric parameters are listed in Table 1. Both **1*M*** and **1*P*** optimized to C_2 symmetry, while the X-ray structure of **1*M*** is very close to C_2. Generally, there is good agreement between the X-ray structure and the B3LYP computed geometry; the major exception is the $C_1'-C_1\alpha$ distance, where the X-ray experimental distance appears to be too short.

The computed geometries of the two isomers of **1** are very similar except for the dihedral angle about the disulfide, where it is −90.1° in **1*M*** and +87.1° in **1*P***. Otherwise, their bond distances differ by less than 0.01 Å and their bond angles differ by less than 2.5°. In agreement with the X-ray study and the conformational analysis, we find that the preferred isomer is **1*M***; it lies 1.22 kcal mol^{-1} below **1*P***.

(18) Bachrach, S. M.; Woody, J. T.; Mulhearn, D. C. *J. Org. Chem.* **2002**, *67*, 8983−8990.
(19) Waring, P.; Beaver, J. *Gen. Pharmac.* **1996**, *27*, 1311−1316.
(20) Bernardo, P. H.; Chai, C. L. L.; Deeble, G. J.; Liu, X.-M.; Waring, P. *Bioorg. Med. Chem. Lett.* **2001**, *11*, 483−485.
(21) Olmstead, W. N.; Brauman, J. I. *J. Am. Chem. Soc.* **1977**, *99*, 4219−4278.
(22) (a) Becke, A. D. *J. Chem. Phys.* **1993**, *98*, 5648−5650. (b) Lee, C.; Yang, W.; Parr, R. G. *Phys. Rev. B* **1988**, *37*, 785−789. (c) Vosko, S. H.; Wilk, L.; Nusair, M. *Can. J. Phys.* **1980**, *58*, 1200−1211. (d) Stephens, P. J.; Devlin, F. J.; Chabalowski, C. F.; Frisch, M. J. *J. Phys. Chem.* **1994**, *98*, 11623−11627.
(23) (a) Chandrasekhar, J.; Andrade, J. G.; Schleyer, P. v. R. *J. Am. Chem. Soc.* **1981**, *103*, 5609−5612. (b) Saunders, W. H., Jr. *J. Phys. Org. Chem.* **1994**, *7*, 268−271. (c) Merrill, G. N.; Kass, S. R. *J. Phys. Chem.* **1996**, *100*, 17465−17471.
(24) Cramer, C. J. *Essentials of Computational Chemistry. Theories and Models*; John Wiley: Chichester, UK, 2002.
(25) Frisch, M. J.; Trucks, G. W.; Schlegel, H. B.; Scuseria, G. E.; Robb, M. A.; Cheeseman, J. R.; Zakrzewski, V. G.; Montgomery, J. A. J.; Stratmann, R. E.; Burant, J. C.; Dapprich, S.; Millam, J. M.; Daniels, A. D.; Kudin, K. N.; Strain, M. C.; Farkas, O.; Tomasi, J.; Barone, V.; Cossi, M.; Cammi, R.; Mennucci, B.; Pomelli, C.; Adamo, C.; Clifford, S.; Ochterski, J.; Petersson, G. A.; Ayala, P. Y.; Cui, Q.; Morokuma, K.; Malick, D. K.; Rabuck, A. D.; Raghavachari, K.; Foresman, J. B.; Cioslowski, J.; Ortiz, J. V.; Baboul, A. G.; Stefanov, B. B.; Liu, G.; Liashenko, A.; Piskorz, P.; Komaromi, I.; Gomperts, R.; Martin, R. L.; Fox, D. J.; Keith, T.; Al-Laham, M. A.; Peng, C. Y.; Nanayakkara, A.; Gonzalez, C.; Challacombe, M.; Gill, P. M. W.; Johnson, B.; Chen, W.; Wong, M. W.; Andres, J. L.; Gonzalez, C.; Head-Gordon, M.; Replogle, E. S.; Pople, J. A. *GAUSSIAN-98*, A.7; Gaussian, Inc.: Pittsburgh, PA, 1998.
(26) (a) Laur, P. H. *Steric aspects of sulfur chemistry*; Senning, A., Ed.; Dekker: New York, 1972; Vol. 3, pp 91−274. (b) Boyd, R. J.; Perkyns, J. S.; Ramani, R. *Can. J. Chem.* **1983**, *61*, 1082−1085. (c) Qian, W.; Krimm, S. *Biopolymers* **1992**, *32*, 321−326.
(27) Donzel, B.; Kamber, B.; Wüthrich, K.; Schwyzer, R. *Helv. Chim. Acta* **1972**, *55*, 947−961.
(28) Strickland, R. W.; Richardson, F. S. *J. Chem. Soc., Perkin Trans. 2* **1976**.
(29) Mitra, A. K.; Chandrasekaran, R. *Int. J. Peptide Protein Res.* **1977**, *10*, 235−239.
(30) Varughese, K. I.; Lu, C. T.; Kartha, G. *Int. J. Peptide Protein Res.* **1981**, *18*, 88−102.

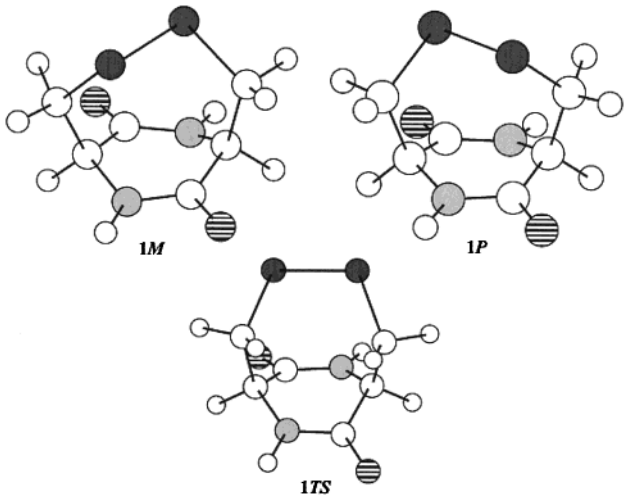

FIGURE 1. Optimized geometries of **1*M***, **1*P***, and **1*TS***. Carbon is indicated by a large empty circle, hydrogen by a small empty circle, sulfur by a dark circle, nitrogen by a light circle, and oxygen by a striped circle.

TABLE 1. Parameters of 1

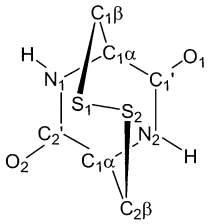

	1*M*		**1*P***	**1*TS***
parameter[a]	B3LYP	X-ray	B3LYP	B3LYP
S_1-S_2	2.084	2.019	2.086	2.134
$S_1-C_1\beta$	1.840	1.819, 1.818	1.844	1.842, 1.834
$C_1\beta-C_1\alpha$	1.552	1.561, 1.537	1.551	1.575, 1.572
$C_1'-C_1\alpha$	1.536	1.448, 1.458	1.530	1.535, 1.538
$C_1\alpha-N_1$	1.456	1.456, 1.470	1.461	1.454, 1.462
$C_1'-N_2$	1.363	1.383, 1.366	1.360	1.364, 1.361
$C_1'-O$	1.224	1.233, 1.229	1.225	1.225, 1.221
$S_2-S_1-C_1\beta$	104.2	103.7, 103.9	104.9	110.5, 107.0
$S_1-C_1\beta-C_1\alpha$	116.6	114.0, 114.9	117.5	122.7, 115.6
$C_1\alpha-C_1'-N_2$	115.8	117.5, 116.9	115.4	114.3, 113.9
$C_1\alpha-N_1-C_2'$	123.8	121.5, 119.4	126.2	124.1, 124.5
$C_2\beta-S_2-S_1-C_1\beta$	−90.1	−94	87.1	29.2
$C_2\alpha-C_2'-N_1-C_1\alpha$	−18.2	−10	−5.1	5.1, 1.6
ΔE	0.0		1.26	18.53
ΔG	0.0		1.22	17.59

[a] Distances in Å, angles in deg, and energies in kcal mol^{-1}.

We located the transition state for the interconversion of the two isomers, shown in Figure 1 as **1*TS***. Geometrical parameters are listed in Table 1. This transition state is reached primarily by rotation about the $C_1\alpha-C_1\beta$ bond. The barrier height is 17.59 kcal mol^{-1}, suggesting that the isomers will very slowly interconvert at room temperature. **1*TS*** has no symmetry. Optimization of a transition-like geometry with C_2 symmetry results in a structure having two imaginary frequencies and is 25.31 kcal mol^{-1} above **1*M***.

TABLE 2. Geometric Parameters for Structures along the Reaction Paths

structure	$S_{nuc}-S$	$S-S_{lg}$	$S_{nuc}-S-S_{lg}$
1*M*		2.084	
1*M*-*ID*	4.729	2.087	
1*M*-*TS1*	3.589	2.129	167.4
1*M*-*INT*	2.691	2.356	172.0
1*M*-*TS2*	2.158	3.511	171.7
1-*PROD*	2.095	5.116	
1*P*		2.085	
1*P*-*ID*	5.444	2.087	
1*P*-*TS1*	3.780	2.115	159.7
1*P*-*INT*	2.628	2.405	171.5
1*P*-*TS2*	2.151	3.395	174.1

TABLE 3. Relative Energies (kcal mol^{-1}) for Structures along the Reaction Paths

structure	ΔG_{rel}	structure	ΔG_{rel}
1*M* + HS^-	0.0	**1*P*** + HS^-	1.22 (0.0)[a]
1*M*-*ID*	−16.48	**1*P*-*ID***	−14.55 (−15.77)
1*M*-*TS1*	−6.84	**1*P*-*TS1***	−1.31 (−2.53)
1*M*-*INT*	−10.24	**1*P*-*INT***	−4.07 (−5.29)
1*M*-*TS2*	−2.69	**1*P*-*TS2***	0.54 (−0.68)
1-*PROD*	−6.16	**1-*PROD***	−6.16 (−7.38)

[a] Free energies relative to **1*P*** + HS^- are in parentheses.

Reaction of 1 with HS^-. We examined nucleophilic attack of thiolate at sulfur in both **1*M*** and **1*P***. Important geometric parameters for the critical points along the reactions are listed in Table 2, their relative free energies are listed in Table 3, and their structural representations are given in Figure 2.

The first step is the formation of an ion−dipole complex, which we label as **1*M*-ID** and **1*P*-ID**. These two structures are local energy minima but may not be global minima structures. We did not perform an exhaustive search but rather started the search with the thiolate group positioned 3.5 Å from one sulfur and collinear with the S−S bond. These ion dipoles should thus be thought of as representative of the actual ion−dipole complex with a relative energy close to that of the lowest energy ion dipole structure. In both ion−dipole complexes, the thiolate anion bridges the amide proton and the adjacent methine proton. The two structures are quite similar, except for the dihedral about the S−S bond. In **1*M*-*ID***, the sulfur atoms are positioned toward the nitrogen, while in **1*P*-*ID*** they are near the carbonyl group. This difference accounts for the differing $S-S_{nuc}$ distances in the two ion−dipole complexes.

The next step of the reaction involves the thiolate group attacking sulfur by swinging toward the disulfide group. The entering transition states are labeled as **1*M*-*TS1*** and **1*P*-*TS1***. Both transition states are quite early, as indicated by the S−S distances. In **1*M*-*TS1***, the $S_{nuc}-S$ distance is 3.589 Å, while the $S-S_{lg}$ distance is only 0.04 Å longer than in the reactant. Similarly, in **1*P*-*TS1***, the $S-S_{nuc}$ distance is very long (3.780 Å) and the $S-S_{lg}$ distance has lengthened only by 0.03 Å from reactant. The attack of the thiolate is not collinear, as we have seen in all of our other studies of nucleophilic attack at sulfur.[10,11,15,16]

1*M*-*TS1* is 9.64 kcal mol^{-1} above **1*M*-*ID*** and 6.84 kcal mol^{-1} below the reactants. The barrier is larger for the

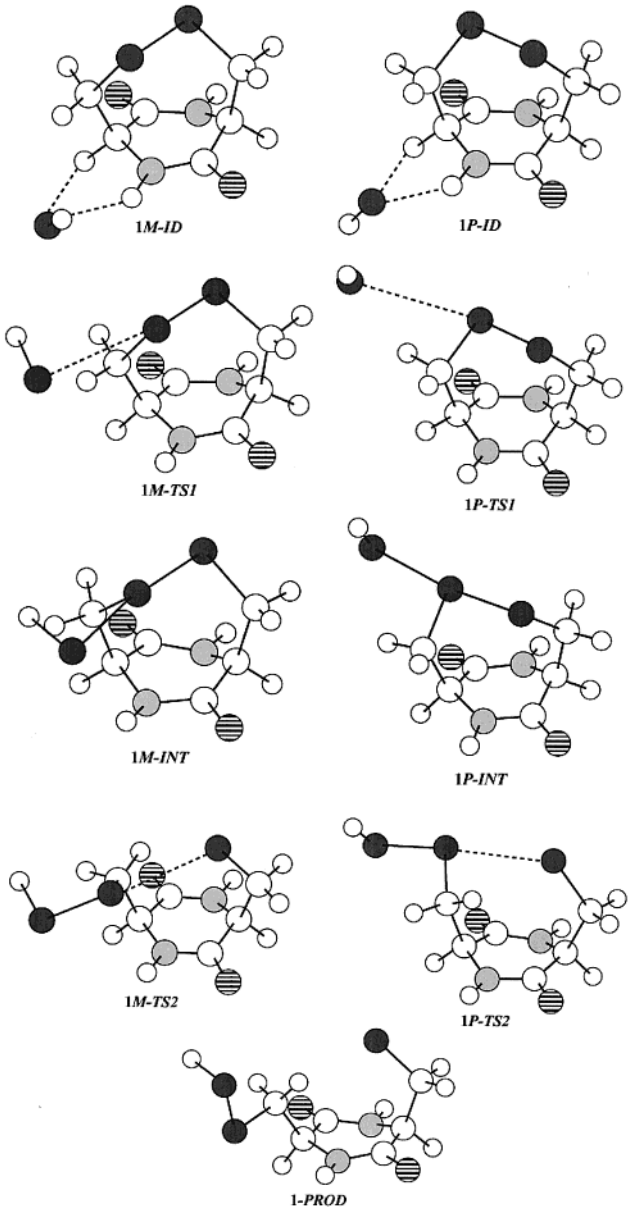

FIGURE 2. Optimized geometries of critical points for the reaction of thiolate with **1*M*** and **1*P***. See Figure 1 for legend.

other pathway; **1*P*-*TS1*** is 13.24 kcal mol^{-1} above **1*P*-*ID***. The approach of thiolate to the disulfide bond in **1*M*** takes it near the amide nitrogen and proton, a region of favorable electrostatic attraction. On the other hand, thiolate must approach the disulfide of **1*P*** near the carbonyl oxygen atoms, bringing on electrostatic repulsion between these two negative charged groups.

Thiolate continues in toward the disulfide, forming next a local intermediate. These two intermediates, **1*M*-*INT*** and **1*P*-*INT***, are characterized by nonequivalent S−S distances. In both intermediates, the S_{nuc}−S distance (2.691 Å in **1*M*-*INT***, 2.628 Å in **1*P*-*INT***) is longer than the S−S_{lg} distance (2.356 Å in **1*M*-*INT***, 2.405 Å in **1*P*-*INT***). The S−S−S angle is close to linear.

1*M*-*INT* lies 10.24 kcal mol^{-1} below reactants, though still above **1*M*-*ID***. As in **1*P*-*ID***, the electrostatic interaction between S_{nuc} and the carbonyl group destabilizes

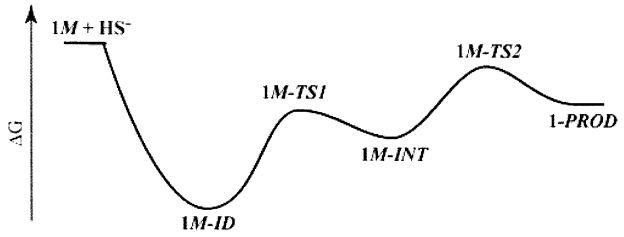

FIGURE 3. Reaction coordinate diagram for the reaction of **1*M*** + thiolate.

1*P*-*INT* relative to the ***M*** isomer. It is 6 kcal mol^{-1} higher in energy than **1*M*-*INT*** and is 5.29 kcal mol^{-1} below reactants (**1*P*** + HS$^-$).

Our study of nucleophilic substitution of cyclic disulfides indicated that the mechanism is dependent upon the strain energy of the ring. The sulfur in strained rings cannot create a bond to the nucleophile and maintain the ring; therefore, these rings cleave concomitantly with attack of the nucleophile—an S_N2 mechanism. However, sulfur in relatively strain-free rings can maintain the ring while forming a new bond to the nucleophile, leading to a stable intermediate along the nucleophilic substitution pathway. The bicyclic nature of **1** is sufficiently free of strain so as to allow the formation of the hypercoordinate sulfur intermediate.

The next step in the reaction involves the cleavage of the S−S_{lg} bond and the full formation of the S_{nuc}−S bond. In the transition states for this process (**1*M*-*TS2*** and **1*P*-*TS2***), the S−S_{lg} distances have lengthened by over 1 Å from the intermediates, while the S_{nuc}−S distances are about 2.15 Å, only slightly longer than for a typical S−S bond.

The barrier for this second step is 7.55 kcal mol^{-1} from **1*M*-*INT***, but this transition state still lies 2.69 kcal mol^{-1} below the reactants. The barrier is less (4.61 kcal mol^{-1}) leading from **1*P*-*INT***; it lies just below the energy of the reactants. The barrier for the ***P*** path is lower here due to the relief of the electrostatic repulsion between the S_{nuc} and the carbonyl oxygen, since this transition includes a component of rotation about the C_α−C_β bond that increases their separation.

A number of possible conformations of the product are possible. We report here the lowest energy conformation we located, **1-*PROD***. Notice that this is the product for both reaction of **1*M*** and **1*P***. This structure benefits from a weak intramolecular hydrogen bond between the sulfur anion and a hydrogen on C_β across the ring. Overall, the reaction is exergonic, $\Delta G = -6.16$ kcal mol^{-1} from **1*M*** and −7.38 kcal mol^{-1} from **1*P***.

A sketch of the reaction coordinate diagram is given in Figure 3. The surface is characterized by three wells: the ion−dipole complex, the intermediate, and the product. The presence of a stable intermediate negates the S_N2 mechanism. Clearly, this reaction proceeds by the addition−elimination mechanism, consistent with our previous gas-phase results for simple acyclic and cyclic disulfides.[10,11,18] The bicyclic system **1** is sufficiently strain-free that the sulfur can accommodate the formation of an additional bond, creating the hypercoordinate stable intermediate that defines the A−E process.

The model system studied here embeds the disulfide bond within a protein-like environment. The computa-

tions therefore suggest that gas-phase nucleophilic substitution at sulfur in proteins and gliotoxin will occur by the addition−elimination mechanism. Extension of these computations to the solution phase is underway.

Acknowledgment. The support of grants from the Robert A. Welch Foundation (W-1442) and the Petroleum Research Fund, administered by the American Chemical Society, are gratefully acknowledged.

Supporting Information Available: Coordinates of all optimized B3LYP/6-31+G* structures, their absolute energies, and number of imaginary frequencies. This material is available free of charge via the Internet at http://pubs.acs.org.

JO034046X